American Journal of Pathology, Vol. 166, No. 1, January 2005

Immunopathology and Infectious Disease

Early Events in the Pathogenesis of Eastern Equine Encephalitis Virus in Mice

Peter Vogel,* Wayne M. Kell,* David L. Fritz,* Michael D. Parker,† and Randal J. Schoepp*‡

From the Divisions of Pathology, Virology†, and Diagnostic Systems,‡ United States Army Medical Research Institute of Infectious Diseases, Fort Detrick, Frederick, Maryland*

To elucidate the pathogenesis of eastern equine encephalitis (EEE) virus infections, we used histopathology, immunohistochemistry, and *in situ* hybridization to track the spread and early cellular targets of viral infection in mice. Young mice were inoculated with virulent EEE virus in their right rear footpad and were followed in a time-course study for 4 days. Virulent EEE virus produced a biphasic illness characterized by an early self-limiting replication phase in peripheral tissues followed by an invariably fatal central nervous system (CNS) phase. In the early extraneural phase, there was primary amplifying replication of virus within fibroblasts at the inoculation site and within osteoblasts in active growth areas of bone that resulted in a transient high-titer viremia. Pathological changes and viral infection were observed as early as 12 hours post-infection (PI) in osteoblasts, skeletal muscle myocytes, and in fibroblasts along fascial sheaths. The severity and extent of infection in peripheral tissues peaked at day 1 PI. In the neural phase of infection, virus was first detected in the brain on day 1 PI, with rapid interneuronal spread of infection leading to death by day 4 PI. EEE virus appeared to be directly cytopathic for neurons. The very rapid onset and apparently random and widely dispersed infection in the CNS, with concurrent sparing of olfactory neuroepithelium, strongly suggests that invasion of the CNS by EEE occurs by a vascular route, rather than via peripheral nerves or the olfactory neuroepithelium. Our finding that metaphyseal osteoblasts are an early site of amplifying viral replication may explain the higher-titer viremias and higher incidence of neuroinvasion and fulminant encephalitis seen in the young, and may also explain why mature animals become refractory to encephalitis after peripheral inoculation with EEE virus. *(Am J Pathol 2005, 166:159–171)*

Eastern equine encephalitis (EEE) virus is a single-stranded RNA virus in the genus *Alphavirus* (family *Togaviridae*) that can cause a severe mosquito-borne encephalitis in humans, horses, and game birds.[1] In North America, EEE virus is prevalent in freshwater swamps along the Atlantic and Gulf coasts of the United States where both its mosquito vector, *Culiseta melanura*, and its passerine bird reservoir hosts live.[2] The virus has a very wide host range, but as *Culiseta* mosquitoes rarely feed on mammalian hosts, other bridging mosquito species actually transmit the virus from infected birds to horses, and occasionally, to humans. Most EEE infections in humans are inapparent or produce a low-grade fever followed by malaise, arthralgia, and myalgia. However, in some cases, EEE virus crosses the blood-brain barrier and causes a severe, and often fatal, acute encephalitis, which kills 50 to 75% of infected humans and leaves many survivors with serious neurological sequelae.[1,3] It has long been recognized that EEE infection in children tends to have a more rapid onset and to be more severe. Goldfield et al reported that one in eight young children developed fulminant encephalitis and only 1 in 23 had an inapparent infection.[4] Similarly, EEE tends to be more severe in elderly patients.[5] Histologically, infection in the human central nervous system (CNS) is characterized by a diffuse meningoencephalitis with widespread neuronal necrosis, perivascular cuffing with polymorphonuclear neutrophils and mononuclear cells, and vasculitis with vessel occlusion.[6] The neuropathology of virulent EEE has been investigated in several species,[7–9] including experimentally infected laboratory mice.[10–13] However, time-course studies that apply *in situ* hybridization (ISH) and immunohistochemistry (IHC) to track the progression of viral infection in extraneural tissues at early time points have not been reported.

The purpose of this study was to investigate the early events in the pathogenesis of EEE virus infection in mice because the early viral cell targets and the interactions between viral replication, virus-specific immune responses, and nonspecific defenses in the pathogenesis

Accepted for publication September 20, 2004.

Address reprint requests to Peter Vogel, Lexicon Genetics, Inc, 8800 Technology Forest Place, The Woodlands, TX 77381-1160. E-mail: pvogel@lexgen.com.

of virulent EEE are still not well defined. It is likely that the initial events after *Alphavirus* infections play a critical role in determining the overall severity and eventual outcome of disease. A better understanding of the early cell targets of EEE virus may contribute to our understanding of virus pathogenesis and to the development of more effective vaccines and viral therapeutics.

Materials and Methods

Virus Strain

The pathogenic EEE virus strain, FL91–4679, was originally isolated from *Aedes albopictus* mosquitoes collected in Florida in 1991 and had been passaged once in suckling mice, three times in Vero cells, and twice in BHK-21 cells.[14] We propagated virus on BHK-21 cell monolayers maintained in Eagle's minimal essential medium (EMEM) containing 10% fetal bovine serum (FBS). Viral titers in mouse blood samples and viral stocks were measured by plaque assay in Vero cells maintained in EMEM containing 5% FBS.

Mice

Specific pathogen-free, 5-week-old C57BL/6 female mice (National Cancer Institute, Frederick, MD) were maintained in a biosafety level 3 (BSL-3) facility and were housed in microisolator cages and provided water and standard mouse chow *ad libitum*. This research was conducted in compliance with the Animal Welfare Act and other federal statutes and regulations relating to animals and experiments involving animals and in adherence to principles stated in the Guide for the Care and Use of Laboratory Animals (Committee on Care and Use of Laboratory Animals of the Institute of Laboratory Animal Resources, National Research Council, NIH Publication No. 86–23, revised 1996, NRC Publication, 1996 edition). All procedures were reviewed and approved by the USAMRIID Laboratory Animal Care and Use Committee, and performed in a facility accredited by the Association for Assessment and Accreditation of Laboratory Animal Care, International.

Experimental Design

Beginning at 12 hours post-infection following subcutaneous inoculation of virus into the footpad, we collected tissues from infected mice and examined them for histopathological lesions and for virus distribution using immunohistochemistry and *in situ* hybridization methods. Briefly, lightly anesthetized mice ($n = 24$) (Metofane; Pitman-Moore, Mundelein, IL) were inoculated in the subcutis of the right footpad with 10^5 plaque-forming units (PFU) of EEE virus (FL91–4679) in 0.025 ml of Hanks' balanced salt solution (HBSS) diluent. Negative control mice ($n = 12$) were inoculated with HBSS diluent alone. At 12 hours and 1, 2, and 4 days post-inoculation (PI), four randomly selected virus-infected mice and two negative control mice were bled from the retroorbital sinus for virus isolation and then killed by inhalation of CO_2. After death, the mice were immediately perfused via the left ventricle with 20 ml of 10% buffered formalin, and then tissues were immersed in formalin fixative for 7 days. The tissues collected included brain, lung, tracheobronchial lymph nodes, heart, thymus, heart, trachea, thyroid gland, parathyroid gland, pituitary gland, uterus, ovary, vagina, urinary bladder, kidney, adrenal gland, submandibular salivary glands and lymph nodes, liver, pancreas, spleen, esophagus, stomach, duodenum, jejunum, ileum, colon, mesenteric lymph nodes, head (three levels), left and right legs and feet, and left and right popliteal lymph nodes. The draining popliteal lymph nodes were dissected from the right and left rear legs, and both the legs and skull were decalcified in 10% EDTA (Sigma Chemical Co., St. Louis, MO) in Tris buffer solution (pH 6.95). All tissues were embedded in paraffin, sectioned at 5 μm, and mounted on positively charged glass slides (Superfrost Plus, Fisher Scientific, Pittsburgh, PA). Histopathological evaluation of hematoxylin and eosin stained (H&E) sections was completed and the presence of viral antigens or viral RNA was detected in serial tissue sections by immunohistochemistry and *in situ* hybridization, respectively.

Immunohistochemistry

A broadly cross-reactive polyclonal rabbit antibody produced against alphaviruses (kindly provided by Cindy Rossi, USAMRIID, Fort Detrick, Frederick, MD) was diluted 1:30,000 in PBS (pH 7.4) and used as primary antibody to detect viral antigens. The DAKO EnVision System (DAKO Corporation, Carpinteria, CA) was used as an amplification and reporter system. The assay was modified for use on a DAKO Autostainer Universal Staining System. Briefly, tissue sections were deparaffinized and rehydrated. To increase staining intensity, an antigen-retrieval procedure requiring immersion of sections in citrate buffer for 30 minutes at 97°C was used. Endogenous peroxidases were blocked by incubation in 0.03% hydrogen peroxide. Tissue sections were incubated with the appropriate dilution of primary rabbit antibody followed by the secondary antibody, horseradish peroxidase-labeled polymer conjugated to goat anti-rabbit immunoglobulins. Staining was completed by adding the substrate-chromagen, diaminobenzidine (DAB). All samples were incubated in a humidified chamber at room temperature (25 to 27°C). Tissues were counterstained with hematoxylin, dehydrated, and cleared, and coverslips were applied with Permount (Fisher Scientific). Negative controls included substitution of normal rabbit serum for the primary antibody. Sections of confirmed EEE virus-infected mouse brain were used as a positive control.

In Situ *Hybridization*

An EEE-reactive cDNA probe consisting of the 3′ one-third of the EEE virus genome, encoding the viral structural proteins was cloned into the pBluescript plasmid (Stratagene, La Jolla, CA). Negative-control probes consisted of plasmid without genomic viral sequence inserts. All probes were labeled with digoxigenin-11-dUTP by

nick translation and tissue sections were processed as previously described.[15] Sections were deparaffinized and rehydrated before immersion in 2X SSC (1X SSC = 0.15 mol/L NaCl + 0.015 mol/L Na citrate, pH 7.0) for 10 minutes at 70°C. The tissue sections were then incubated with 20 μg/ml of proteinase K (Boehringer Mannheim, Indianapolis, IN) in Tris-buffered saline (TBS: 0.05 mol/L Tris-HCl, 150 mmol/L NaCl, 1 mmol/L $MgCl_2$, pH 7.6) at 37°C for 30 minutes in a humid chamber. Digoxigenin (DIG)-labeled probe DNA was denatured at 95°C for 5 minutes and chilled rapidly at −20°C for 1 minute. Standard hybridization solution contained 45% (v/v) deionized formamide (Ambion, Austin, TX), 10% dextran sulfate (Amresco, Solon, OH), 4X SSC, 2 mg/ml of bovine serum albumin (BSA; Boehringer Mannheim), 25 ng of nick-translated plasmid probe, and nuclease-free water in a total volume of 50 μl. Hybridization buffer was added to the denatured probe and mixed, and 50 to 100 μl of the probe mixture was placed on each tissue section. Coverslips were applied and sections were incubated overnight in a humid chamber at 37°C. After hybridization, sections were washed twice for 5 minutes each with 1X SSC and then incubated in Tris-buffered saline (TBS) containing 0.1% BSA and 0.1% Triton for 15 minutes at room temperature. DIG probe was detected in tissue sections with a 1:600 dilution of an alkaline phosphatase (AP)-labeled anti-DIG antibody (Boehringer Mannheim) in TBS-0.1% BSA for 60 minutes at 37°C in a humid chamber. The AP-labeled sections were stained by incubation with freshly prepared BCIP/NBT (5-bromo-4-chloro-3-indolyl phosphate) as substrate with 4-nitro blue tetrazolium chloride as chromagen (Gibco BRL, Rockville, MD) in Tris-buffered saline (100 mmol/L Tris-HCl, 100 mmol/L NaCl, 50 mmol/L $MgCl_2$, pH 9.5) at 37°C. Endogenous AP activity was blocked by adding 1 mmol/L levamisol (Vector Laboratories, Burlingame, CA) to the enzyme substrate solution. Stained slides were washed in deionized water, counterstained with nuclear fast red (Vector Laboratories), dehydrated, and coverslips were applied with Permount (Fisher Scientific).

Results

Viremia and Clinical Course of EEE Infections

Of the time points sampled, titers of EEE virus (FL91–4679) were highest at 12 hours post-infection (PI). Titers declined at later time points but low levels of virus were still detectable at 4 days PI (Table 1). By day 1 PI, the FL91–4679-inoculated mice were lethargic and had ruffled fur. By day 4 PI, the clinical signs had progressed in severity to hunching, tremors, and prostration, at which time all surviving mice were killed.

Table 1. Viremia (log_{10} PFU/ml) at Various Times Post-Infection of C57BL/6 Mice Inoculated in the Right Footpad with 10^5 PFU of FL91–4679

EEE, FL91–4679	12 hours	1 day	2 days	4 days
	6.15	6.20	3.64	2.70
	6.32	6.20	NT	2.81
	6.58	5.30	4.71	2.00
	6.56	6.54	3.79	3.23
Average	**6.44**	**6.24**	**4.31**	**2.87**
HBSS control	0	0	0	0

NT, not tested.

EEE Virus Localization and Associated Histopathological Lesions

12 Hours PI

IHC demonstrated diffuse extracellular granular deposits between subcuticular collagen bundles and within macrophages at the site of injection, suggesting that only a fraction of the infectious dose reached the circulation. Staining for EEE virus antigen and nucleic acid was intracytoplasmic and finely granular in most cell types, although coarse granules or prominent clumps were present in macrophages in the subcutis of the foot and in draining lymph nodes. In the draining popliteal lymph node, the strong staining for viral antigen (but minimal-to-absent staining for RNA) in subcapsular sinus macrophages and dendritic cells suggested trapping of viral particles draining from the inoculation site. The numerous virus-positive (by both IHC and ISH) cells were located primarily along fascial planes surrounding muscles and nerves, and along tendon sheaths (Figure 1A). Many of the elongated virus-positive cells appeared to be perivascular, perineural, perimysial and peritendonous fibrocytes, and fibroblasts. Other widely scattered virus-positive cells in the subcutaneous connective tissues appeared to be macrophages and fibrocytes. Multifocally, numerous virus-positive cells were clustered in the fibrous attachments of muscle to bone (Figure 1B). Rarely, there was strong positive staining of synovial cells lining joint spaces (Figure 1C). In the draining popliteal lymph node of all four mice, there were one to several small clusters of virus antigen-positive dendritic cells located at the periphery of the node lining the subcapsular sinus (Figure 1D) and superficial lymphoid follicles. In addition, there were scattered subcapsular sinus macrophages containing minimal amounts of finely stippled immunoreactive viral antigen. There were sometimes a few necrotic cells associated with the infected cell foci. Only very weak staining for viral nucleic acids was detected in serial sections of the draining lymph nodes.

In the long bones, although most osteoblasts appeared to be normal, there were rare apoptotic cells lining the bony trabeculae in the metaphyseal regions (Figure 1E). In all four mice, there was intense staining of histologically normal osteoblasts in the lateral metaphysis and periosteum of the femur and tibia (Figure 1, F to H). On the contralateral leg, there were also ISH- and IHC-positive clusters of osteoblasts in the metaphyses of long bones of all four mice, and along the metaphyseal periosteum in two of four mice. No viral antigen or nucleic acid was detected in the draining popliteal lymph node of the contralateral leg. Elsewhere, rare virus-positive cells were present multifocally in the bones of the nasal turbinates, hard palate, and skull. There were rare ISH- and

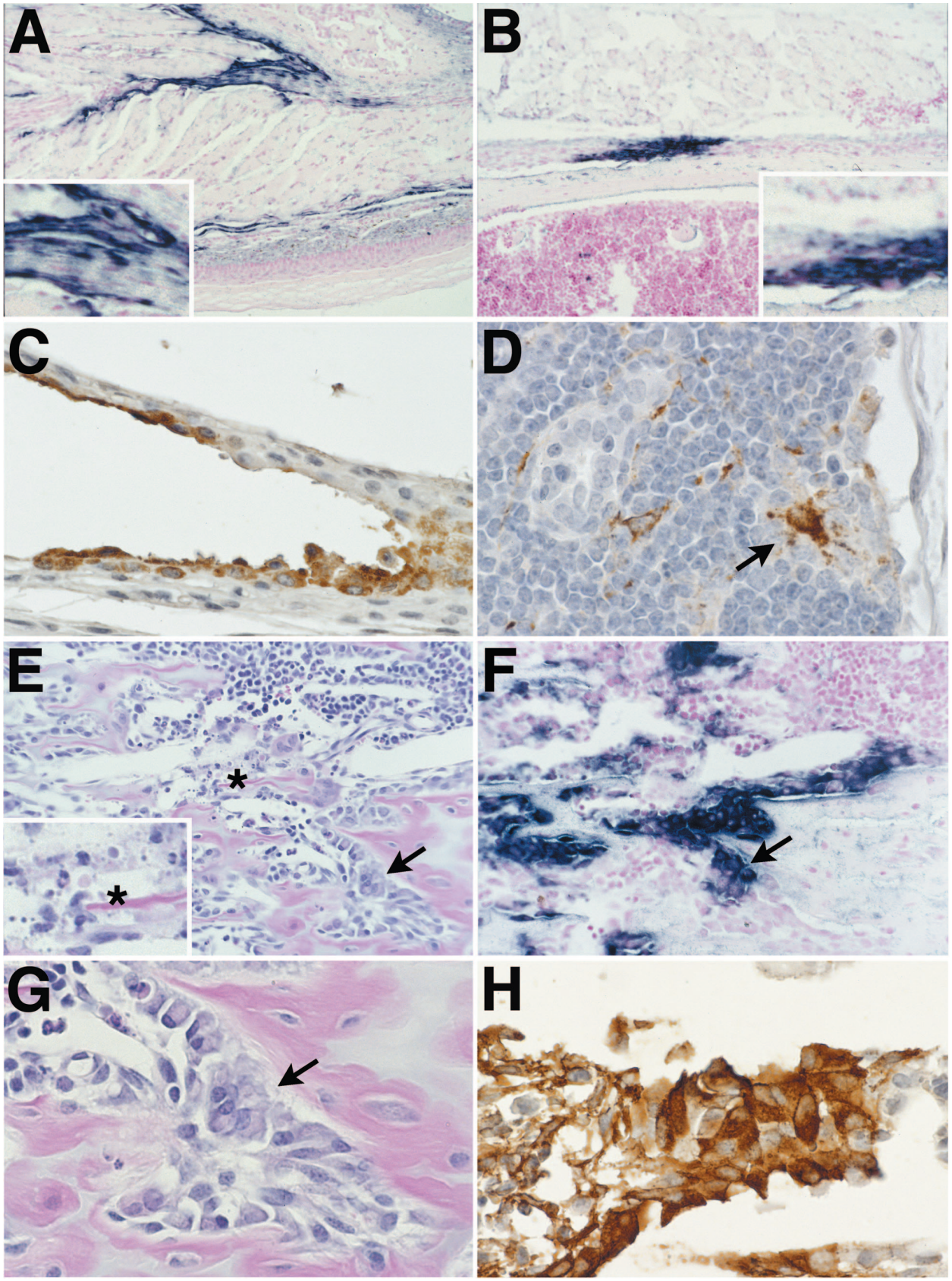
A
B
C
D
E
F
G
H

IHC-positive ovarian stromal and internal thecal cells in all four mice examined.

Day 1 PI

A single cluster of virus-positive neurons located in the somatosensory cortex of one mouse provided the first evidence of CNS invasion. The numbers of viral antigen and nucleic acid-positive fibrocytes/fibroblasts in the subcutis and located along tendons and in the perivascular and perimyseal connective tissue sheaths also increased by day 1 PI. Epineurial and epimysial cells were frequently virus-positive and there were also a few clusters of virus-positive cells in the cutaneous squamous epithelium. Significantly, the many viral antigen-positive macrophages in the footpad were uniformly negative by ISH. In the femur and tibia, there was widespread necrosis and loss of osteoblasts and other cells in the areas immediately adjacent to the growth plate, with associated viral antigen-positive macrophages and cell debris in affected areas. By ISH, the most intensely stained osteoblasts were located along the diaphysis, with markedly decreased ISH signal in the areas of the epiphysis and metaphysis that contained necrotic osteoblasts. Viral infection had spread to the osteoblasts and fibroblasts in the connective tissues encircling the growth plate. These included the ring of fibrous tissue and bone comprising the perichondrial ring of LaCroix and the ossification groove of Ranvier (Figure 2A). Although the cells within the fibrous connective tissues of the periosteum and ring of Ranvier were morphologically normal at 24 hours PI (Figure 2C), these cells were intensely positive by ISH (Figure 2D) and IHC. By this time, there was also intense ISH-positive staining of fibroblasts and periosteum at insertion sites of tendons on bone (Figure 2E). In the draining popliteal lymph node, there were scattered apoptotic/necrotic cells in the subcapsular and medullary sinuses, and associated sinusoidal macrophages contained cell debris and variable amounts of granular viral antigen (Figure 2B). However, ISH of serial sections again showed that these sinus macrophages were negative for viral nucleic acids.

In the contralateral leg, there was necrosis and loss of osteoblasts in numerous foci in the metaphysis, with abundant viral antigen detected in the osteoblasts, macrophages, and cell debris in these areas. The most intense ISH signal was seen in periosteal osteoblasts and in some small clusters of endosteal osteoblasts. Metabolically active chondrocytes and osteoclasts at the growth plate were apparently refractory to infection, as were osteocytes and small osteoblasts in other areas. Also in the contralateral leg, were scattered virus-positive fibroblasts/fibrocytes located at tendon insertions and multifocally within muscle sheaths. Significantly, virus-positive subcutaneous fibrocytes in the footpad and synovial cells of the contralateral leg were not detected.

Elsewhere, there were scattered necrotic cells in bones and tooth pulp, with virus-positive cells including the osteoblasts lining the marrow cavities of turbinate and skull bones, the odontoblasts and fibroblastic cells in the dental pulp (Figure 2F), and even the basal epithelium of a vibrissa in one mouse. There were also small numbers of weakly positive myocytes in the ventricular myocardium as well as clusters of virus-positive cells in the ovarian stroma and in a few foci in the fallopian tubes and in the myometrium.

Day 2 PI

Virus-infected neurons were detected in the CNS of three of four mice. The location of the virus-infected neurons in the CNS was highly variable, with one mouse having a few virus-positive neurons at the base of the cerebellum and a single Purkinje cell, but numerous scattered positive granular cell neurons. There were also virus-infected layer I piriform cortical neurons on one side with minimal extension to layer II neurons, and a few positive neurons within the lateral olfactory tract on one side. In another mouse, we found a cluster of virus-positive neurons in the caudate putamen in addition to a couple of isolated virus-positive neurons in the cerebral cortex. In the third mouse, there were scattered virus-positive neurons in the piriform cortex, and clusters of virus-positive neurons in the secondary motor cortex and caudate putamen.

At the inoculation site, there were numerous antigen-positive but ISH-negative macrophages in the connective tissues. ISH signal in the inoculated footpad was present in fascial fibroblasts, subepithelial fibroblasts, and some myocytes. By day 2 PI, the metaphyseal areas were essentially negative for EEE virus antigen and nucleic acid and abundant necrotic cells and debris were present in the areas of trabecular bone normally lined by osteoblasts. ISH demonstrated the apparent direct extension of infection from the periosteum to surrounding myocytes. In addition, small numbers of keratinocytes stained positively for both viral antigen and nucleic acid. These individual and small groups of virus-positive keratinocytes usually appeared as a thin band of cells below the stratum corneum. In the draining popliteal lymph node, there was a diffuse moderate lymphoid hyperplasia with a few weakly antigen-positive (but ISH-negative) macrophages in the subcapsular sinuses.

Figure 1. Representative photomicrographs showing lesions and virus distribution in selected tissues at 12 hours post-infection (PI). Eastern equine encephalitis (EEE) virus-infected cells are stained for viral RNA by *in situ* hybridization (ISH) (**A**, **B**, and **F**) and EEE viral antigen by immunohistochemistry (IHC) (**C**, **D**, and **H**). **A:** ISH-positive fibroblasts (**inset**) and macrophages in the dermis and connective tissue fascia in the inoculated foot. **B:** ISH-positive tendon at insertion on bone. Inset shows higher power view of virus-positive cells. **C:** IHC-positive synovial cells in metatarsal joint of inoculated foot. **D:** IHC-positive dendritic macrophages (**arrow**) in draining popliteal lymph node. **E:** Metaphysis of distal femur stained with H&E demonstrates the normal appearance of most osteoblasts lining the primary spongiosa (**arrow**) and the rare apoptotic cells (**inset**, **asterisk**) in EEE virus-infected mouse. **F:** Note the ISH-positive osteoblasts lining the primary spongiosa in this sequential section of area shown in **D**. The intensity of ISH signal is reduced in the area of necrosis. **G:** Higher magnification of area shown in **E** and **F**, showing the normal morphology and numbers of the virus-positive osteoblasts covering trabeculae. **H:** IHC staining of sequential section of the same area demonstrating EEE virus antigen in morphologically osteoblasts.

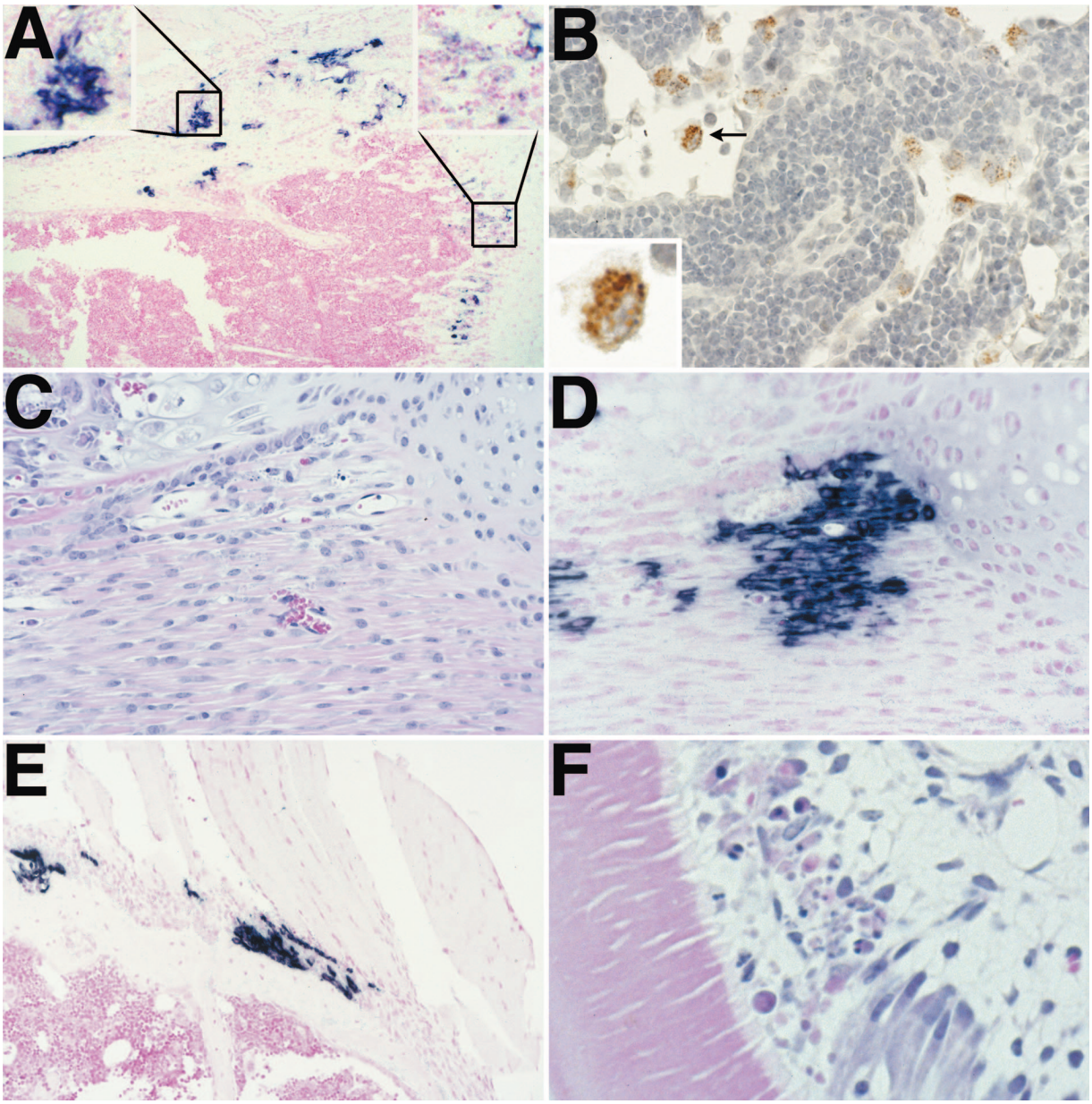

Figure 2. Representative photomicrographs showing lesions and virus distribution in selected tissues at 1 day post-infection (PI). Eastern equine encephalitis (EEE) virus infected cells are stained for viral RNA by *in situ* hybridization (ISH) (**A**, **D** and **E**) and EEE viral antigen by immunohistochemistry (IHC) (**B**). **A:** ISH of proximal tibia showing intense staining within the periosteum and ring of Ranvier (**top left inset**). Note the relatively less intense staining of osteoblasts along the growth plate (**top right inset**) at this time point. **B:** IHC of draining popliteal lymph node demonstrates presence of viral antigen in sinus macrophages only. The clumped granular appearance of viral antigen is shown in the inset. At this time point, these macrophages were negatively stained for viral RNA. **C:** This H&E-stained section demonstrates the normal morphology of cells within the fibrous connective tissues of the periosteum and ring of Ranvier. **D:** Note the numerous ISH-stained cells in this sequential section of the area shown in **C**. **E:** At this time point, there was intense ISH-positive staining of fibroblasts and periosteum at insertion sites of tendons on bone. **F:** H&E of tooth. Note the focal disruption and necrosis of odontoblasts.

In other locations, there was multifocal necrosis and loss of odontoblasts, ameloblasts, and tooth pulp in all four mice. In affected areas, there was segmental loss of the odontoblast cell layers and multifocal necrosis and loss of ameloblasts with consequent disruption of normal histological arrangements of the tooth. There were also some perivascular virus-positive foci within the marrow cavities of the bones of the skull in three of four mice. In one mouse, there was a single focus of virus-positive cells under the olfactory epithelium while in two of the four mice there were small clusters of weakly positive myocardial cells. In one mouse, four virus-positive fibroblast cells were detected in the renal medullary interstitium

Day 4 PI

All six remaining mice inoculated with the wild-type virus showed clinical signs of severe neurological disease by day 4 PI and were killed. Histologically, there was widespread necrosis of neuronal cells and some associated rarefaction of adjacent neuropil and white tracts in all six mice. Generally, the inflammatory cell

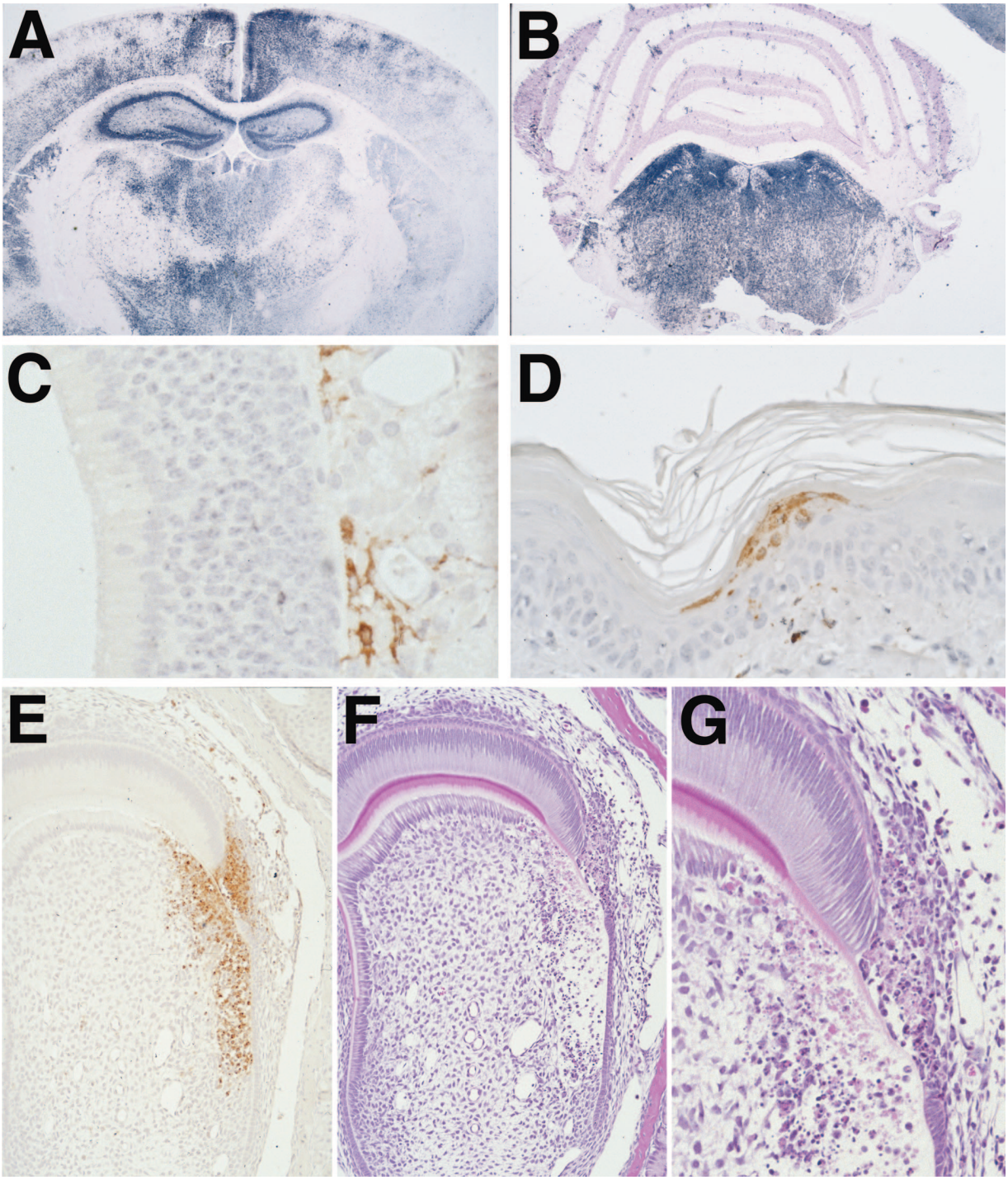

Figure 3. Representative photomicrographs showing lesions and virus distribution in selected tissues at 4 days post-infection (PI. Eastern equine encephalitis (EEE) virus-infected cells are stained for viral RNA by *in situ* hybridization (ISH) (**A** and **B**) and EEE viral antigen by immunohistochemistry (IHC) (**C**, **D**, and **E**). **A:** ISH of brain shows the diffuse viral infection of cortex, hippocampus, caudate putamen, and thalamus. **B:** ISH of cerebellum and midbrain of same mouse shows the relative sparing of the cerebellum. **C:** IHC of olfactory mucosa. Note the absence of viral antigen within the olfactory neuroepithelium and the virus-positive cells and processes in the submucosa. **D:** IHC showing virus-positive keratinocytes in skin. **E** and **F:** Sequential sections of a developing tooth stained by IHC and H&E method demonstrates abundant viral antigen in an area of necrosis and disruption in the enamel and dentin layers of the tooth. **G:** Higher magnification of **F** showing necrotic odontoblasts and ameloblasts in the virus-infected area of tooth.

reaction was very mild, consisting mainly of neutrophils and eosinophils. Virus was found chiefly within the perikaryon and dendrites of neurons in the cerebral cortex and midbrain, although some glial cells were also virus-positive. In the hippocampus, lesions were more prominent in the gyrus dentatus than the pyramidal hippocampus. Scattered Purkinje cells and associated cerebellar granular layer neurons became virus-positive relatively late in disease. Virus-positive neurons were located within the caudate putamen, middle layers of the

cerebral cortex, internal nuclei, pyramidal cortex, and multifocally in the frontal, cingulate, and parietal cortex and most brainstem nuclei (Figure 3A). The strongest signal was often detected in the thalamus, caudate putamen, and pons. Notably, the intensity of viral staining was diminished in areas with diffuse neuronal necrosis. Viral infection was essentially absent in the internal and external capsules, pyramidal tract, hippocampal commisure, lateral olfactory tract, cerebellar peduncles, and corpus callosum. The pyramidal neurons of the ventrolateral CA3 field of hippocampus were usually involved. Except for the polymorph layer, the dentate gyrus of the hippocampus was generally spared. Involvement of the cerebellum was generally less severe than that seen in the cerebrum and brainstem (Figure 3B), and generally consisted of variably sized foci of virus-positive Purkinje cells and their associated granular cell neurons. In terminally ill mice, there were scattered large clusters of virus-infected Purkinje cells (Figure 4H). In all six mice, there was necrosis in the olfactory tubercle and multifocally in the piriform cortex, and IHC and ISH staining for virus was most intense in the granular cell layer of the olfactory bulbs, with variable extension to the plexiform and glomerular cell layers.

Significantly, there was minimal involvement of the olfactory neuroepithelium, consisting only of a small amount of virus-specific staining in a few isolated olfactory neurons, and in a few individual cells located beneath the olfactory neuroepithelium (Figure 3C) and within perisinusoidal nerves in the nasal turbinates surrounding the vomeronasal organs. In all six mice, virus infection in the eyes typically involved multiple foci in the retinal ganglion cell layer with extensions to the internal and external granular layers.

At the inoculation site, there were numerous viral antigen-positive myocytes, fibroblasts, and macrophages, as well as several clusters of intraepithelial cells and rare sebaceous glands in the footpad. In both legs, there were rare antigen-positive macrophages and fibroblasts in the periosteum and within the ring of Ranvier. Viral nucleic acid was only detected in occasional widely scattered skeletal muscle myocytes. In developing teeth, there was necrosis of odontoblasts and ameloblasts that disrupted the dentin and enamel layers (Figure 3, E and G). In affected areas, there were clusters of virus-positive odontoblasts and ameloblasts and scattered individual positive cells in the dental pulp (Figure 3F).

By day 4 PI, the lesions in the bones of EEE virus-infected mice were characterized by widespread necrosis and loss of osteoblasts, with accompanying thickening of the epiphyseal growth plate and elongation of the primary spongiosa (Figures 4, A and B). At the epiphyseal growth plate, viral infection induced a marked disruption in the normal process of cartilage maturation and replacement by bone. In uninfected mice, the zone of hypertrophic chondrocytes ranged up to four cells thick (Figure 4C). However, as early as day 1 PI, there was multifocal loss of osteoblasts adjacent to the growth plate and the zone of hypertrophy was doubled in thickness (Figure 4D). By day 4 PI, the growth plate was up to four times the normal thickness, with the severe alterations affecting the regions of hypertrophy, mineralization, and ossification (Figure 4D). The major alterations included elongation of the zone of cartilage hypertrophy in the areas that had lost osteoblasts, and reduced formation of osteoid in the zone of ossification. The persistent and altered hypertrophic chondrocytes and changes in the growth plate were present only in specific areas where virus infection had eliminated metaphyseal osteoblasts and resulted abnormal endochondral ossification. Hypertrophic chondrocyte columns were up to four times the normal length and some of the more mature chondrocytes contained large eosinophilic cytoplasmic granules (Figure 4, F and G). The decreased osteoid on primary trabeculae was associated with severely reduced numbers of osteoblasts along the metaphyseal trabeculae. Other virus-infected tissues in the head sections included sebaceous glands, skeletal muscle, and epithelial cells. Lesions in the heart involved rare individual and clustered myocytes with increased cytoplasmic eosinophilia, disruption of striations, and increased granularity of sarcoplasm. Affected cardiomyocytes were invariably antigen-positive but ISH-negative. In the thymic cortex, multifocal lymphocytic apoptosis was present around tingible body macrophages but viral signal was absent. In skin, widely scattered foci of virus-infected keratinocytes were now located primarily within the stratum corneum and only the most superficial layer of the adjacent stratum granulosum was also virus-positive (Figure 3D). Widespread apoptosis of lymphocytes was present in the spleen, peripheral lymph nodes, and Peyer's patches, but without associated viral antigen or nucleic acids. In the kidneys, there were scattered clusters of virus-positive cells (IHC and ISH) in the medulla. The virus-positive cells were located between the renal tubules, arranged in columns, and had broad flat cytoplasmic extensions (Figure 4I).

Discussion

The early interactions between EEE virus and the host are critically important in determining whether the eventual

Figure 4. Representative photomicrographs showing lesions and virus distribution in selected tissues at 4 days post-infection (PI). **A:** Low magnification photomicrograph of proximal femur of uninfected control mouse. Note the normal thickness of cartilage and bone trabeculae in the primary spongiosa of the metaphysis. **B:** Low magnification photomicrograph showing the growth plate of an eastern equine encephalitis (EEE) virus infected mouse on day 4 PI. Note the increased thickness of the zone of hypertrophic cartilage and the very thin and elongated fibrous trabeculae adjacent to the growth plate. **C:** Higher magnification photomicrograph of normal growth plate demonstrates that the zone of hypertrophic chondrocytes is only up to four cells thick, and abundant osteoblasts are located at the bone-cartilage interface and along the primary spongiosa. **D:** This section shows typical changes in growth plate at day 1 PI. Osteoblasts are generally absent from the growth plate area and the zone of hypertrophic chondrocytes is already up to eight cells thick. **E:** At day 4 PI, the zone of hypertrophy is up to 15 cells thick. **F:** High magnification photomicrograph showing the morphology of normal chondrocytes in the hypertrophic zone of uninfected control mouse. **G:** High magnification showing unusual large eosinophilic cytoplasmic granules within the most basal hypertrophic chondrocytes. **H:** ISH showing extension of viral infection to Purkinje cells in the cerebellum of moribund mice on day 4 PI. **I:** IHC demonstrating viral antigen within sustentacular cells in the renal papilla.

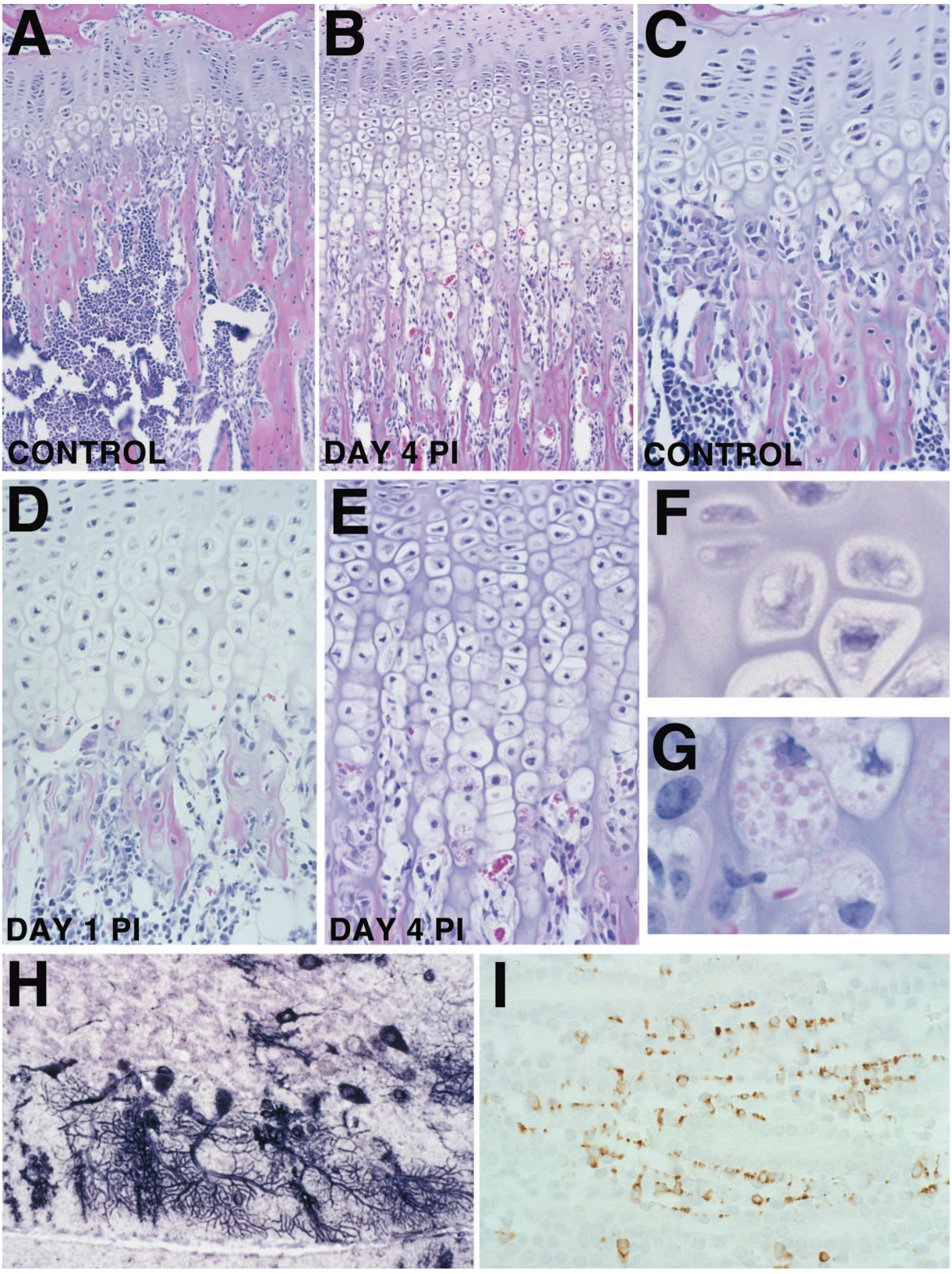
A
CONTROL
B
DAY 4 PI
C
CONTROL
D
DAY 1 PI
E
DAY 4 PI
F
G
H
I

outcome of virus infection is a mild subclinical syndrome or lethal fulminant encephalitis. In this study, we used *in situ* hybridization and immunohistochemistry to detect EEE virus RNA and proteins, respectively, to identify the early cell targets and events involved in the pathogenesis of EEE infection. We interpreted the simultaneous presence of both viral antigen and viral nucleic acids within the same cell type to indicate viral replication. We found that EEE virus infection follows the typical pattern reported in other *Alphavirus* encephalitides,[1] with initial viral replication near the inoculation site and hematogenous spread to permissive cells in other peripheral tissues during the early phase of infection. In most alphaviral encephalitides, both viral replication in peripheral tissues and viremia levels have already subsided before the second CNS phase of infection, when high levels of virus RNA and antigens are found primarily within CNS neurons.

The subcutaneous inoculation of virulent virus into one footpad mimicked the natural transmission of EEE by a mosquito vector and allowed us to determine the early cell targets of EEE infection by tracking the infection in the inoculated hind foot and leg and comparing virus distribution in the opposite leg. The ability to compare virus distribution in both legs permitted us to distinguish genuine viral tropisms (eg, osteoblasts, fibroblasts, and skeletal muscle) from apparent artifacts of direct inoculation (synovium and macrophages). In this way, we discovered several remarkable features of early EEE infection that were not previously known or predicted. Alphaviruses have a wide host range that includes both invertebrate (mosquito) and vertebrate (birds and mammals) but an unexpected finding of this study was the extensive early replication of EEE virus in active osteoblasts, which appear to play a previously unrecognized but critical role in the pathogenesis of the disease. Other novel targets of EEE infection that we identified include ovarian stromal cells, skin keratinocytes, and renal medullary interstitial cells. At later time points, viral nucleic acid and antigen were also found in the skeletal and cardiac myocytes, developing teeth, skin epithelium, ovaries, and renal papilla.

At the earliest time point (12 hours PI), local viral replication at the inoculation site was suggested by the presence of EEE viral RNA and antigen within fibroblasts lining facial planes in the footpad. Disseminated viral replication was also evident, with EEE viral antigen and nucleic acid detected within dendritic cells of the draining popliteal lymph node and within osteoblasts at the bone growth plates. Although apoptosis of lymphocytes was not a major feature of EEE infection, the weak staining for viral RNA in dendritic cells of the draining lymph node implied that some viral replication had occurred in these cells.

Osteoblast Infection

As early as 1936, Hurst[16] noted that the levels of EEE viremia were higher than could be accounted by measured titers in the viscera or muscle and dermis at the inoculation site, and he hypothesized "that the virus must multiply chiefly either in the blood or in some tissue intimately connected with the blood stream and forming only a small part by weight of the various viscera." This study is the first to show that osteoblasts are a major cellular target of EEE virus after subcutaneous inoculation and are the cells responsible for the high virus titers seen after infection. We believe that osteoblasts represent the primary site of EEE virus amplification, and that the central role of these cells may explain the increased susceptibility of the young to developing fulminant encephalitis. The rapid spread of infection to bone was clearly demonstrated by the appearance of virus-positive osteoblasts at the tibial and femoral growth plates of both legs of all mice as early as 12 hours PI. Histopathological changes in affected areas were not evident until 24 hours PI, but the pyknosis, karyorrhexis, cytoplasmic eosinophilia, and fragmentation of osteoblasts suggests a direct virus-induced cytocidal effect. Infection of the osteoblasts lining the trabeculae in this area was probably enhanced by the slow blood flow in metaphyseal capillaries. The areas of bone with less active bone formation and remodeling were infrequently affected, suggesting that metabolically active osteoblasts are more susceptible or permissive to EEE infection than resting bone cells.

Lesions in the long bones were present only in specific areas where viral infection had eliminated metaphyseal osteoblasts, and were characterized by abnormal endochondral ossification and marked thickening of the growth plate. In our study, we found that chondrocytes failed to undergo normal apoptosis in areas where osteoblasts were absent. Apparently, the loss of osteoblasts led to persistence of hypertrophic chondrocytes at the growth plate and interfered with the usual endochondral ossification processes.

Our findings support the hypothesis that osteoblasts may be involved in the process of vascular invasion into the hypertrophic cartilage zone and the apoptosis of terminal hypertrophic chondrocytes. Calcification of the matrix surrounding hypertrophic chondrocytes precedes and contributes to the death of hypertrophic chondrocytes.[17] Although capillary invasion is necessary for ossification, it is unknown whether apoptosis of hypertrophic chondrocytes is the stimulus for capillary growth or if capillary invasion is the trigger for chondrocyte apoptosis. Osteoblasts produce VEGF in response to a variety of stimuli[18–20] and their absence after EEE infection could account for the persistence of hypertrophic chondrocytes and observed growth plate disturbances. The large cytoplasmic inclusions we observed in the persistent chondrocytes probably represent matrix vesicles that are normally released by chondrocytes near the base of the hypertrophic zone during chondrocyte apoptosis.[21]

The tendency to develop encephalitis after infection is also age-dependent in humans, with adults being much more resistant than infants and young children.[22] The increased susceptibility of young animals and humans to clinically apparent alphaviral encephalitis[5] has been attributed to age-dependent factors in neurons that suppress viral replication and/or virus-induced apoptosis.[23,24] To some extent, the age-related virulence correlates with ability of CNS neurons to replicate virus

and undergo apoptotic cell death. Immature developing neurons support complete viral replication but as neuronal populations and circuits mature in the postnatal brain, viral infection becomes progressively restricted and nonproductive. One possible mechanism for increased resistance with increasing age is that mature neurons are resistant to virus-induced apoptosis because they express cellular inhibitors of apoptosis.[23] Maturation of the host is clearly important to the development of age-dependent resistance to alphaviral infections but studies have not shown the increased resistance to be caused by enhanced interferon or humoral and cellular immune responses in older mice.[23,25] The central role of metabolically active osteoblasts in amplifying EEE virus infection may explain the increased susceptibility of young mice to fulminant EEE encephalitis. Early comparative pathology studies clearly showed that young mice are more prone to developing lethal encephalitis, but the underlying reasons for this increased susceptibility were not determined.[26–28] Direct age-related changes in neuronal susceptibility to EEE virus are not likely because mice become refractory only to peripheral, not intracerebral inoculation of EEE as they get older.[27,28] We attribute the increased resistance of older mice to peripherally inoculated EEE virus to the markedly reduced population of metabolically active (and thus virus amplifying) osteoblasts in adult mice. In contrast to the strong age-dependent susceptibility to EEE virus encephalitis, mature mice apparently remain equally susceptible to Venezuelan equine encephalitis (VEE) virus encephalitis after extraneural inoculation.[27] We hypothesize that the continued susceptibility of older mice to peripheral VEE infections is due to the continued presence of permissive amplifying host cells (olfactory neuroepithelium, dendritic cells, and lymphoid tissue[29]) in adult mice.

CNS Infection

One objective of this study was to determine the most likely route of entry of EEE virus into the CNS after subcutaneous inoculation. Commonly recognized routes of viral neuroinvasion include: the vascular route, with virus crossing the blood-brain barrier by passive transfer across endothelium, by active infection of endothelium, or by transport within infected leukocytes into the CNS; neurogenic spread by axonal transport along peripheral nerves; and invasion via the olfactory tract, after initial infection of olfactory neuroepithelial cells.[30] In this study, the pattern of invasion within the brains of EEE-infected mice was very different from that previously reported in VEE encephalitis, where the virus initially infects the olfactory neuroepithelium during the early viremic phase and then spreads to other areas of the CNS via the olfactory tract and limbic structures.[31] In contrast, the very rapid, multifocal, and apparently random pattern of EEE infection of the CNS suggests a hematogenous route of neuroinvasion. Our findings corroborate early studies in which virus appeared first in the brain rather than in the spinal cord and spinal ganglia after inoculation in the hind leg and the findings that intrasciatic inoculation was no more neuroinvasive than intradermal inoculation and removal of olfactory bulbs did not prevent early infection.[16] We hypothesize that EEE virions cross the blood-brain barrier by passive transfer or within infected leukocytes because we did not detect viral antigen or RNA in endothelial cells in the CNS or any other neural tissue. Our findings support earlier electron microscopy studies that localized EEE virions to virtually every type of cell in the brain except capillary endothelial cells.[12] Neurogenic spread to the CNS from peripheral nerves is unlikely given the very rapid (24 hours PI) appearance of infected neurons in multiple locations within the cerebral cortex and the late appearance of infection in the brainstem and cerebellum. An additional finding of our study is that the olfactory tract was not an important route of neuroinvasion. Infected neuroepithelial cells were not detected until late in the infection and these were most likely infected via retrograde transport from the CNS. Of course, the limited sensitivity of the immunohistochemistry and *in situ* hybridization assays we used would probably not detect low-level replication within olfactory neuroepithelium. Thus our finding that EEE virus administered subcutaneously did not infect olfactory neuroepithelium to an appreciable degree does not guarantee that a large dose of aerosolized EEE would not be neuroinvasive via the olfactory neuroepithelium.

Other Cell Targets

As noted previously, osteoblasts appear to be the major peripheral site of EEE virus amplification after subcutaneous inoculation, but several other cell types also support viral replication. The initial cell type that supports viral replication at the inoculation site was not determined with certainty, but the morphology and locations of the infected cells in the connective tissue cells suggest that they are fibroblasts and fibrocytes, and that infection normally spreads from these cells to adjacent myocytes by direct contact. In addition to osteoblasts and fibroblasts/fibrocytes, we identified viral RNA and antigen in skeletal muscle, cardiac muscle, tooth odontoblasts and ameloblasts, renal medullary interstitial cells, ovarian stromal cells, skin epithelium, and possibly dendritic cells. The scattered distribution of clusters of virus-infected cells in the connective tissues and epithelium suggests that virus was initially disseminated hematogenously to susceptible cells, but that secondary spread was restricted to cells that were in direct contact with infected cells. We previously noted the sequential spread of infection from metaphyseal osteoblasts to endosteal and periosteal osteoblasts and fibroblasts along the diaphysis of the bone. Similarly, EEE infection in the skeletal muscles of the legs was initially confined to individual or small clusters of fibers in close apposition to tendon insertions on bone. The sequential course of infection suggests that viral infection spread to the myocytes from periosteal and connective tissue fibroblasts. The early restriction of viral spread by cell-to-cell contact suggests that nonspecific responses may be involved in controlling the spread of infection. Although antibody responses are critically important in clearing *Alphavirus* infection from

the CNS,[32,33] the reduction in viral replication in peripheral tissues occurs too rapidly to be explained by adaptive, antigen-specific immune responses and is thus more likely due to innate, nonspecific responses to viral infections (such as type 1 interferon production). Recent studies have shown that an active type-I interferon system controls viral replication and spread in extraneural tissues.[34,35]

The renal interstitium contains an elaborate network of stellate sustentacular cells, which represent a highly specialized type of fibroblast. In the medulla, these interstitial cells have thick cytoplasmic processes that support the walls of the urinary tubules and the vasa recta.[36] Recently, EEE virus antigen was detected in fusiform and stellate cells in the renal medullary interstitium of horses and it was proposed that the cells might be infected antigen-presenting dendritic cells, macrophages, fibroblasts, or myofibroblasts.[8] The morphology and location of the virus-infected cells in the kidneys of our mice were consistent with those described for renal medullary interstitial cells and the presence of both EEE antigen and RNA in these cells suggests that these medullary interstitial cells support viral replication.

The transient infection of clusters of skin epithelial cells may also be due to interferon responses. Because viral infection was never detected in the stratum germinativum, we suspect that basal epithelial cells do not support viral replication and that infected dendritic Langerhans cells carry the virus to permissive cells in the stratum granulosum where the infection spreads to adjoining permissive epithelial cells. In this instance, continued diffuse spread of virus in the superficial layers of the skin may be prevented by local interferon responses, or by the failure of keratinocytes to release infectious virions, and/or by the inability of maturing (keratinizing) epithelial cells to maintain viral replication.

In conclusion, we found that EEE virus spreads and replicates rapidly in peripheral tissues after subcutaneous inoculation. This study is the first to show that the active osteoblast is probably the primary cell target and site of viral amplification for EEE virus after subcutaneous inoculation. Our findings suggest that that EEE virus preferentially entered the CNS via the blood stream rather than the olfactory tract or retrograde flow through peripheral nerves. Other previously unreported EEE targets include the ovarian stromal cells, skin keratinocytes, renal medullary sustentacular cells, odontoblasts, ameloblasts, and dental pulp elements. Although extrapolations from mouse models to humans must be made with caution, the central role of active osteoblasts in the early pathogenesis EEE in these mice may provide an explanation for the increased tendency of the young to develop fulminant encephalitis. Identifying the EEE virus receptor on osteoblasts might be used to develop improved live, attenuated vaccines and antiviral therapeutics.

Acknowledgments

We thank L. Miller, P. Fogle, and R. Moxley for their excellent technical assistance.

References

1. Calisher CH: Medically important arboviruses of the United States and Canada. Clin Microbiol Rev 1994, 7:89–116
2. Scott TW, Weaver SC: Eastern equine encephalomyelitis virus: epidemiology and evolution of mosquito transmission. Adv Virus Res 1989, 37:277–328
3. Deresiewicz RL, Thaler SJ, Hsu L, Zamani AA: Clinical and neuroradiographic manifestations of eastern equine encephalitis. N Engl J Med 1997, 336:1867–1874
4. Goldfield M, Sussman O: The 1959 outbreak of Eastern encephalitis in New Jersey: I. Introduction and description of outbreak Am J Epidemiol 1968, 87:1–10
5. McGowan Jr JE, Bryan JA, Gregg MB: Surveillance of arboviral encephalitis in the United States, 1955–1971. Am J Epidemiol 1973, 97:199–207
6. Farber S, Hill A, Connerly M, Dingle J: Encephalitis in infants and children caused by the virus of the eastern variety of equine encephalitis. JAMA 1940, 114:1725–1731
7. Patterson JS, Maes RK, Mullaney TP, Benson CL: Immunohistochemical diagnosis of eastern equine encephalomyelitis. J Vet Diagn Invest 1996, 8:156–160
8. Del Piero F, Wilkins PA, Dubovi EJ, Biolatti B, Cantile C: Clinical, pathologic, immunohistochemical, and virologic findings of eastern equine encephalomyelitis in two horses. Vet Pathol 2001, 38:451–456
9. Pursell AR, Mitchell FE, Seibold HR: Naturally occurring and experimentally induced eastern encephalomyelitis in calves. J Am Vet Med Assoc 1976, 169:1101–1103
10. Ognianov D, Fernandez A: Studies on the pathogenesis of eastern equine encephalomyelitis (EEE) in the mouse after injections of virus. Zentralbl Veterinarmed B 1972, 19:89–93
11. Liu C, Voth DW, Rodina P, Shauf LR, Gonzalez G: A comparative study of the pathogenesis of western equine and eastern equine encephalomyelitis viral infections in mice by intracerebral and subcutaneous inoculations. J Infect Dis 1970, 122:53–63
12. Murphy FA, Whitfield SG: Eastern equine encephalitis virus infection: electron microscopic studies of mouse central nervous system. Exp Mol Pathol 1970, 13:131–146
13. Bastian FO, Wende RD, Singer DB, Zeller RS: Eastern equine encephalomyelitis: histopathologic and ultrastructural changes with isolation of the virus in a human case. Am J Clin Pathol 1975, 64: 10–13
14. Mitchell CJ, Niebylski ML, Smith GC, Karabatsos N, Martin D, Mutebi JP, Craig Jr GB, Mahler MJ: Isolation of eastern equine encephalitis virus from Aedes albopictus in Florida. Science 1992, 257:526–527
15. Kell W, Sheridan-Cuddy L, Vogel P: A nonisotopic in situ hybridization assay with digoxigenin-labeled DNA probes to detect viral RNA in paraffin-embedded tissues. Cell Vision 1997, 4:339–346
16. Hurst E: Infection of the rhesus monkey (Macaca mulatta) and the guinea-pig with the virus of equine encephalomyelitis. J Pathol Bacteriol 1936, 42:271–302
17. Poole AR: The growth plate: cellular physiology, cartilage assembly and mineralization. Cartilage: Molecular Aspects. Edited by Newman S. Boca Raton, CRC Press, 1991, pp 179–211
18. Spector JA, Mehrara BJ, Greenwald JA, Saadeh PB, Steinbrech DS, Bouletreau PJ, Smith LP, Longaker MT: Osteoblast expression of vascular endothelial growth factor is modulated by the extracellular microenvironment. Am J Physiol 2001, 280:C72–C80
19. Schlaeppi JM, Gutzwiller S, Finkenzeller G, Fournier B: 1,25-Dihydroxyvitamin D3 induces the expression of vascular endothelial growth factor in osteoblastic cells. Endocr Res 1997, 23:213–229
20. Wang DS, Yamazaki K, Nohtomi K, Shizume K, Ohsumi K, Shibuya M, Demura H, Sato K: Increase of vascular endothelial growth factor mRNA expression by 1,25-dihydroxyvitamin D3 in human osteoblast-like cells. J Bone Miner Res 1996, 11:472–479
21. Anderson HC: Molecular biology of matrix vesicles. Clin Orthop 1995: 266–280
22. Rennels MB: Arthropod-borne virus infections of the central nervous system. Neurol Clin 1984, 2:241–254
23. Griffin DE, Levine B, Tyor WR, Tucker PC, Hardwick JM: Age-dependent susceptibility to fatal encephalitis: alphavirus infection of neurons. Arch Virol Suppl 1994, 9:31–39
24. Griffin DE, Levine B, Ubol S, Hardwick JM: The effects of alphavirus infection on neurons. Ann Neurol 1994, 35(Suppl):S23–S27

25. Griffin DE: Role of the immune response in age-dependent resistance of mice to encephalitis due to Sindbis virus. J Infect Dis 1976, 133: 456–464
26. Morgan I: Influence of age on susceptibility and on immune response of mice to Eastern equine encephalomyelitis virus. J Exp Med 1941, 150:1383–1398
27. Lennette E, Koprowski H: Influence of age on the susceptibility of mice to infection with certain neurotropic viruses. J Immunol 1944, 49:175–191
28. Brown A, Officer JE: An attenuated variant of Eastern encephalitis virus: biological properties and protection induced in mice. Arch Virol 1975, 47:123–138
29. MacDonald GH, Johnston RE: Role of dendritic cell targeting in Venezuelan equine encephalitis virus pathogenesis. J Virol 2000, 74:914–922
30. Monath TP, Cropp CB, Harrison AK: Mode of entry of a neurotropic arbovirus into the central nervous system: reinvestigation of an old controversy. Lab Invest 1983, 48:399–410
31. Vogel P, Abplanalp D, Kell W, Ibrahim MS, Downs MB, Pratt WD, Davis KJ: Venezuelan equine encephalitis in BALB/c mice: kinetic analysis of central nervous system infection following aerosol or subcutaneous inoculation. Arch Pathol Lab Med 1996, 120:164–172
32. Griffin D, Levine B, Tyor W, Ubol S, Despres P: The role of antibody in recovery from alphavirus encephalitis. Immunol Rev 1997, 159: 155–161
33. Griffin DE, Ubol S, Despres P, Kimura T, Byrnes A: Role of antibodies in controlling alphavirus infection of neurons. Curr Top Microbiol Immunol 2001, 260:191–200
34. Grieder FB, Vogel SN: Role of interferon and interferon regulatory factors in early protection against Venezuelan equine encephalitis virus infection. Virology 1999, 257:106–118
35. White LJ, Wang JG, Davis NL, Johnston RE: Role of alpha/beta interferon in Venezuelan equine encephalitis virus pathogenesis: effect of an attenuating mutation in the 5′ untranslated region. J Virol 2001, 75:3706–3718
36. Takahashi-Iwanaga H: The three-dimensional cytoarchitecture of the interstitial tissue in the rat kidney. Cell Tissue Res 1991, 264: 269–281